

## A SECOND-ORDER BIAS MODEL FOR THE LOGARITHMIC HALO MASS DENSITY

INH JEE<sup>1</sup>, CHANGBOM PARK<sup>2</sup>, JUHAN KIM<sup>3</sup>, YUN-YOUNG CHOI<sup>4</sup>, & SUNGSOO S. KIM<sup>5</sup>

<sup>1</sup>Department of Astronomy, The University of Texas, 1 University Station, C1400, Austin, Texas 78712-0259

<sup>2</sup>School of Physics, Korea Institute for Advanced Study, Heogiro 85, Seoul 130-722, Korea

<sup>3</sup>Center for Advanced Computation, Korea Institute for Advanced Study, Heogiro 85, Seoul 130-722, Korea

<sup>4</sup>Dept. of Astronomy & Space Science, Kyung Hee University, Gyeonggi 446-701, Korea; yy.choi@khu.ac.kr

<sup>5</sup>School of Space Research, Kyung Hee University, Gyeonggi 446-701, Korea

*Draft version June 4, 2018*

### ABSTRACT

We present an analytic model for the local bias of dark matter halos in a  $\Lambda$ CDM universe. The model uses the halo mass density instead of the halo number density and is searched for various halo mass cuts, smoothing lengths, and redshift epochs. We find that, when the logarithmic density is used, the second-order polynomial can fit the numerical relation between the halo mass distribution and the underlying matter distribution extremely well. In this model the logarithm of the dark matter density is expanded in terms of log halo mass density to the second order. The model remains excellent for all halo mass cuts (from  $M_{\text{cut}} = 3 \times 10^{11}$  to  $3 \times 10^{12} h^{-1} M_{\odot}$ ), smoothing scales (from  $R = 5h^{-1}$  Mpc to  $50h^{-1}$  Mpc), and redshift ranges (from  $z = 0$  to 1.0) considered in this study. The stochastic term in the relation is found not entirely random, but a part of the term can be determined by the magnitude of the shear tensor.

*Subject headings:* methods: N-body simulations - methods: numerical - galaxies: halos - cosmology: theory - dark matter - large-scale structure of Universe

### 1. INTRODUCTION

Understanding the formation and distribution of galaxies requires knowledge on initial conditions, effects of gravitational evolution, dark matter halo formation, and galaxy formation in dark halos. The standard paradigm is to adopt Gaussian initial density fluctuations that grow through gravitational instability to form dark matter halos. Galaxies are thought to form and evolve in dark halos, which in turn undergo a series of mergers and accretion (White & Rees 1978). It is therefore expected that the observed galaxy distribution is somewhat different from the halo distribution and also from the underlying matter distribution even though it is popularly assumed to trace the dark matter with a constant bias on very large scales. In many future surveys of galaxy redshifts it is hoped to measure cosmological parameters with a high precision from the galaxy distribution, and it is required to know the relations among matter density field, distribution of dark matter halos and galaxy distribution very accurately.

Cosmological N-body simulation is a useful tool that can be used to find the relation between matter and halo distributions, which we will focus on in this paper. Manera & Gaztanaga (2011) recently studied a local halo bias model using an N-body simulation. They adopted a non-linear, local, deterministic bias model of Fry & Gaztanaga (1993) and Taylor-expanded the halo number density contrast  $n_h$  as a second-order polynomial of the matter fluctuation  $\delta_m$ . The coefficients of the linear and quadratic terms are measured as functions of cubical pixel size and halo mass cut. In this paper we extend their work to obtain a halo bias model that describes the local halo-matter density relation in a more universal way. There are many other studies which adopted this model; Guo & Jing (2009) calculated galaxy bias up to the second order from bispectrum based on this model. Roth & Porciani (2011) applied the Eulerian lo-

cal bias (ELB) model and compared the results between Standard Perturbation Theory (SPT) and simulations. It has proved that SPT is a good theoretical model in predicting the bias at fairly large smoothing scale. However, since the growth of the structure is not deterministic, it cannot provide a full picture in estimating bias. Pollack et al. (2011) used four different probes to estimate bias: smoothed density field, power spectra, bispectra and reduced bispectra. They claimed that the Fourier-space analysis is more reliable since it is free from the mode-mixing problem of the real-space analysis. In this study we applied smoothing scale dependent bias to get rid of this problem.

We first adopt to use the halo mass density instead of the halo number density in the halo bias model. This is because the halo mass density has a much tighter and simpler relation with the underlying matter density than the halo number density (see Fig. 1 in section 3.1 below). Seljak et al. (2009) reported that weighting central halos by their mass can significantly reduce stochasticity relative to the dark matter below the Poisson expectation. Park et al. (2010) showed that the gravitational shear calculated from the halo mass density (calculated from the halo distribution by weighting halos with their mass) has a much tighter relation with the true shear field of dark matter than that from the halo number density (halos are uniformly weighted above a certain mass cut). Observational application of the halo mass-weighting to local density estimation has been already made by Park et al. (2008), with an assumption that luminous galaxy mass is proportional to halo mass (see also Park & Choi 2009, Park & Hwang 2009, Hwang & Park 2009 for more applications).

Second we use the logarithmic density  $\ln(1+\delta)$  instead of the density contrast  $\delta$  in our halo bias model. It turns out that using the logarithmic density allows us to find a very simple analytic bias model that are good for all

smoothing scales, halo mass cuts, and redshifts considered. There have been many suggestions for using the logarithmic density as a model for weakly non-linear density field in cosmology (Cole & Jones 1991; Colombi 1994; Kayo et al. 2001; Neyrinck et al. 2009). Cole & Jones (1991) has proposed to use a lognormal model for the matter distribution evolved from Gaussian initial conditions. They provided astrophysical motivations for considering the lognormal model. In particular, they showed that the mass flow governed by the continuity equation leads the density field to a lognormal distribution in the non-linear regime if the velocity fluctuation is assumed linear. Kayo et al. (2001) showed through a comparison with N-body simulations that the lognormal probability distribution is a useful empirical model for the cosmological density fluctuations, which is insensitive to the shape of the density power spectrum. Neyrinck et al. (2009) found that nonlinearities in the dark matter power spectrum are almost absent when the density is transformed to the log density. They also provided several reasons to use the logarithmic density mapping.

Third, we expand the matter density in terms of the halo density, which is opposite to all previous studies. This is required by the simulation data. The log matter density can be fit excellently by a second-order polynomial of the log halo mass density, not vice versa. A model of the form  $\delta_m = f(\delta_h)$  is in practice useful when  $\delta_h$  is an observed quantity and  $\delta_m$  is the one to be estimated.

As in Manera & Gaztanaga (2011) we restrict our study of the halo biasing in the real configuration space. The effects of the redshift-space distortion will be of practical interest, but an observed distribution of galaxies in redshift space can be first corrected for the fingers-of-god by shrinking massive clusters and groups of galaxies and for the large-scale peculiar velocity by using the second-order perturbation theory (Gramann et al. 1994) before the halo bias model in real space is applied. We will briefly discuss the halo bias in Fourier space in section 5.

## 2. N-BODY SIMULATION

### 2.1. Simulation

The simulation used in this paper is based on the Wilkinson Microwave Anisotropy Probe (WMAP) three-year parameters (Spergel et al. 2007),  $\Omega_\Lambda = 0.762$ ,  $\Omega_m = 0.238$ ,  $\Omega_b = 0.042$ ,  $n_s = 0.958$ ,  $h = 0.732$ , and  $\sigma_8 = 0.761$ , where  $\Omega_\Lambda$ ,  $\Omega_m$ , and  $\Omega_b$  are the density parameter associated with the cosmological constant, matter, and baryon, respectively,  $n_s$  is the slope of the primordial power spectrum, and  $\sigma_8$  is the rms fluctuation of the matter density field smoothed with a  $8 h^{-1}\text{Mpc}$  radius top-hat sphere. The simulation evolved  $2048^3$  cold dark matter particles with mass  $9.6 \times 10^9 h^{-1} M_\odot$ , and the minimum halo mass was  $2.9 \times 10^{11} h^{-1} M_\odot$  (30 particles). Initial conditions were generated on a  $2048^3$  mesh, in accordance with the  $\Lambda\text{CDM}$  power spectrum (Eisenstein & Hu 1998). The physical size of the simulation cube is  $1024 h^{-1}\text{Mpc}$ . The initial epoch of the simulation was  $z = 47$ , and 1880 global time steps were taken until the simulation reaches the present epoch. To increase the spatial dynamic range we use a parallel N-body code made by Dubinski et al. (2003, 2004) which is a merger between a PM code (Park 1990, 1997) and a tree-code (Barnes & Hut 1986).

### 2.2. Dark Halos

Since our study compares the halo distribution with the distribution of the underlying dark matter, the way halos are defined can be a crucial problem. The most widely used method, the friends-of-friend (FoF) algorithm, provides an easy way to identify virialized halo regions using a particle linking length parameter (Audit et al. 1998; Davis et al. 1985). Matching the FoF halos with the observed galaxies is unrealistic because each FoF halo can contain many galaxies. A better model is to use subhalos each of which is assumed to contain one galaxy. In this model galaxy mass or luminosity is assigned to halos with the constraint that the halos with mass above a certain limit have the number density equal to that of the galaxies with stellar mass or luminosity above a certain limit. This one-to-one correspondence model or abundance matching method of galaxy assignment scheme has been shown to be quite successful in describing the observed galaxy distribution (Marinoni & Hudson 2002; Vale & Ostriker 2004, 2006; Shankar et al. 2006; Kim et al. 2008; Gott et al. 2009; Choi et al. 2010).

Below we will show that the matter density field has a much higher correlation with the halo mass density field than the halo number density field. If the subhalo mass is weighted to each halo, the mass density fields of the FoF halos and of the subhalos will be the same and it is not important which halo identification scheme is used.

To identify subhalos, the physically self-bound (PSB) group-finding algorithm developed by Kim & Park (2006) and Kim et al. (2008) is used. The PSB method first finds local particle groups using the FoF algorithm and convert the particle distribution in each group into a density field measured at particle positions using a variable-size Spline kernel. The particles in each group are assigned into subgroups near the density peaks. The subgroup particles are used to redefine the subgroup member particles to identify the tidally stable and gravitationally self-bound subhalos through iteration. The PSB group-finding method has its advantage in resolving halos even in dense environment, and can resolve subhalos down to the gravitational force resolution. It should be noted that subhalos are not substructures of the host halo, but immigrated objects that are not yet disrupted within the host and thus should be resolved and treated separately when individual self-gravitating non-linear objects are to be identified. After finding the FoF halos using a standard linking length, the PSB algorithm is applied to identify subhalos. In each FoF halo the most massive subhalo is named the central or main subhalo, and the rest are called subhalos. In this study, we hereafter use the term ‘halo’ for the both kinds of subhalos.

## 3. MATTER DENSITY-HALO MASS DENSITY RELATION

### 3.1. Halo mass density field

When the spatial clustering of galaxies is studied, traditionally galaxies are uniformly weighted or weighted only according to the selection function. The resulting number density field is used to calculate clustering amplitude statistics such as the two-point correlation function and the power spectrum (Davies & Peebles 1983; Park et al. 1994). The uniform weighting is still widely used to

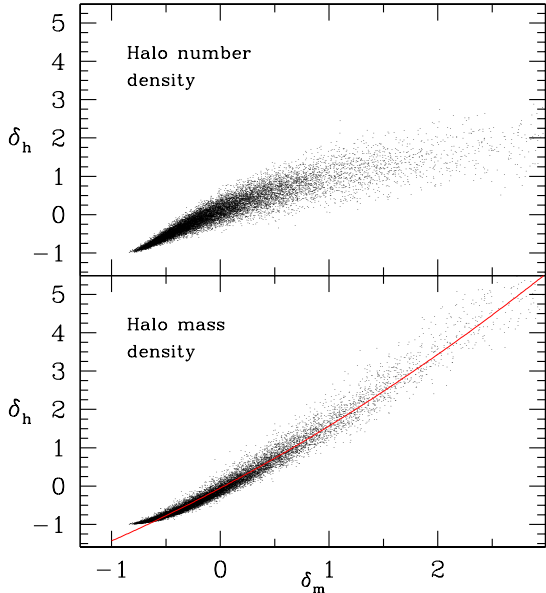


FIG. 1.— The relation of the matter density fluctuation  $\delta_m$  with the halo number density fluctuation (upper panel) and halo mass density fluctuation (lower panel). The relations are obtained on a Gaussian smoothing scale of  $5h^{-1}\text{Mpc}$ . The solid line in the lower panel is a second-order polynomial fit to the data.

study the non-linearity, scale-dependence, and bias in the distribution of galaxies (Tegmark et al. 2006). The main reason for using the uniform weighting is to reduce the shot noise. If galaxy luminosity is used as weight, for example, the resulting luminosity density field is dominated by the rare brightest objects. However, it has been recently shown that the halo mass density field has a much tighter correlation with the underlying matter field than the halo number density field (Park et al. 2010), and the uniform weighting cannot be justified because the bias function of the galaxy number density field is not only more complicated but also less correlated with the matter density field compared to the galaxy mass density field as we show in Figure 1.

In Figure 1 we demonstrate that the halo mass density field has a tighter relation with the matter density field than the halo number density. The  $y$ -axis in the upper panel of Figure 1 is the overdensity in the halo number density, and that in the lower panel is the overdensity in the halo mass density. The density fields are smoothed with a Gaussian filter with radius of  $R = 5h^{-1}\text{Mpc}$ . It can be seen that the halo mass density has a relation with the underlying matter density not only much tighter but also much simpler than the halo number density. The disadvantage of using the number density is even more serious if the FoF halos are used because the number density of the FoF halos is relatively low in high density regions.

### 3.2. The second-order bias model

Even though the relation with the matter density becomes much tighter and simpler when the halo mass density is used, it can not be fit by a low-order polynomial. The line in the lower panel of Figure 1 is a second-order polynomial,  $\delta_h = b_0 + b_1\delta_m + b_2\delta_m^2$ , best fit to the numerical relation. It can be seen that the formula can not fit the data at low densities. We also found that, even if

higher-order terms are added, fitting by a polynomial is not always successful at all redshifts. This reveals a significant limitation of the bias model of Fry & Gaztanaga (1993) working only in a very weak non-linear regime.

We find that, when the logarithmic density is used, a second-order polynomial relation between the halo mass density and the matter density stands almost universally. We first smooth the mass-weighted halo distribution and the matter density field with a Gaussian filter of radius  $R$  and take the logarithm of the resulting smooth density fields  $D = \ln(1 + \delta)$ . The logarithmic transformation can make the result diverge in void regions. Since the smoothing length is always chosen to be equal to or greater than the mean halo separation, the Gaussian smoothing avoid this situation in practice. Note that, when  $|\delta| \ll 1$ ,  $D$  approaches  $\delta$  and our model reduces to the conventional linear bias model. The scatter plots in Figure 2 are the relations between  $D_h = \ln(1 + \delta_h)$  ( $x$ -axis) and  $D_m = \ln(1 + \delta_m)$  ( $y$ -axis) at redshifts  $z = 0$  (left column), 0.5 (middle column), and 1.0 (right column). The smoothing scales are  $R = 5$  (top row), 15 (middle row), and  $50 h^{-1}\text{Mpc}$  (bottom row). Our model for these numerical relations is

$$D_m = \beta_0 + \beta_1 D_h + \beta_2 D_h^2, \quad (1)$$

where  $\beta_i$ 's are functions of the smoothing scale  $R$  and the halo mass cut  $M_{\text{cut}}$ . It should be noted that the matter density is expanded in terms of the halo density. The solid lines in Figure 2 are second-order polynomials best fit to the scatter plots for the halos with mass more than  $3 \times 10^{11} h^{-1} M_\odot$ . For higher mass cuts of  $M_{\text{cut}} = 1 \times 10^{12}$  (long-dashed lines) and  $3 \times 10^{12} h^{-1} M_\odot$  (dotted lines) we show only the best fits without scatter plots to avoid confusion. Since the density fields should be estimated from discrete points like halos or galaxies, the shot noise can be an issue. We choose the smoothing length  $R$  equal to or greater than the mean halo separation to reduce the shot noise. As a result for the halo sample with  $M_{\text{cut}} = 3 \times 10^{11} h^{-1} M_\odot$  ( $\bar{d} = 4.62 h^{-1}\text{Mpc}$ ) we study the halo bias on the scales  $R \geq 4.62 h^{-1}\text{Mpc}$ . Likewise for a sample with  $M_{\text{cut}} = 1$  or  $3 \times 10^{12} h^{-1} M_\odot$  ( $\bar{d} = 6.56$  or  $9.56 h^{-1}\text{Mpc}$ ) the halo bias is studied on scales  $R \geq 6.56$  or  $9.56 h^{-1}\text{Mpc}$ , respectively (see Weinberg et al. 1987 and Park et al. 2005 for choice of the smoothing length for the topology study of galaxy distribution).

### 3.3. Dependence on smoothing scale and halo mass cut

The coefficients  $\beta_i$ 's in Equation (1) depend on smoothing length and halo mass cut. Figure 3 shows the dependence of  $\beta_i$  on  $R$  and  $M_{\text{cut}}$  at three redshifts. In this paper, all the smoothings are done using the Gaussian filter, as stated in section 3.2. The zero-point offset  $\beta_0$  of the halo mass density-matter density relation is significant on small scales, but rapidly vanishes as  $R$  increases. The zero-point off-set is also seen in the  $\delta_m$ - $\delta_h$  relation. On the other hand, the coefficient of the second order term  $\beta_2$  does not decrease much as  $R$  increases, and Equation (1) remain quadratic even on very large scales. Equation (1) can be approximated by a linear bias model  $\delta_h = b_1 \delta_m$  on large scales not because the equation becomes linear but just because the ranges in  $D_h$  and  $D_m$  become small. This can be seen in Figure 2, where the shape of the fitting curves hardly changes as  $R$  increases.

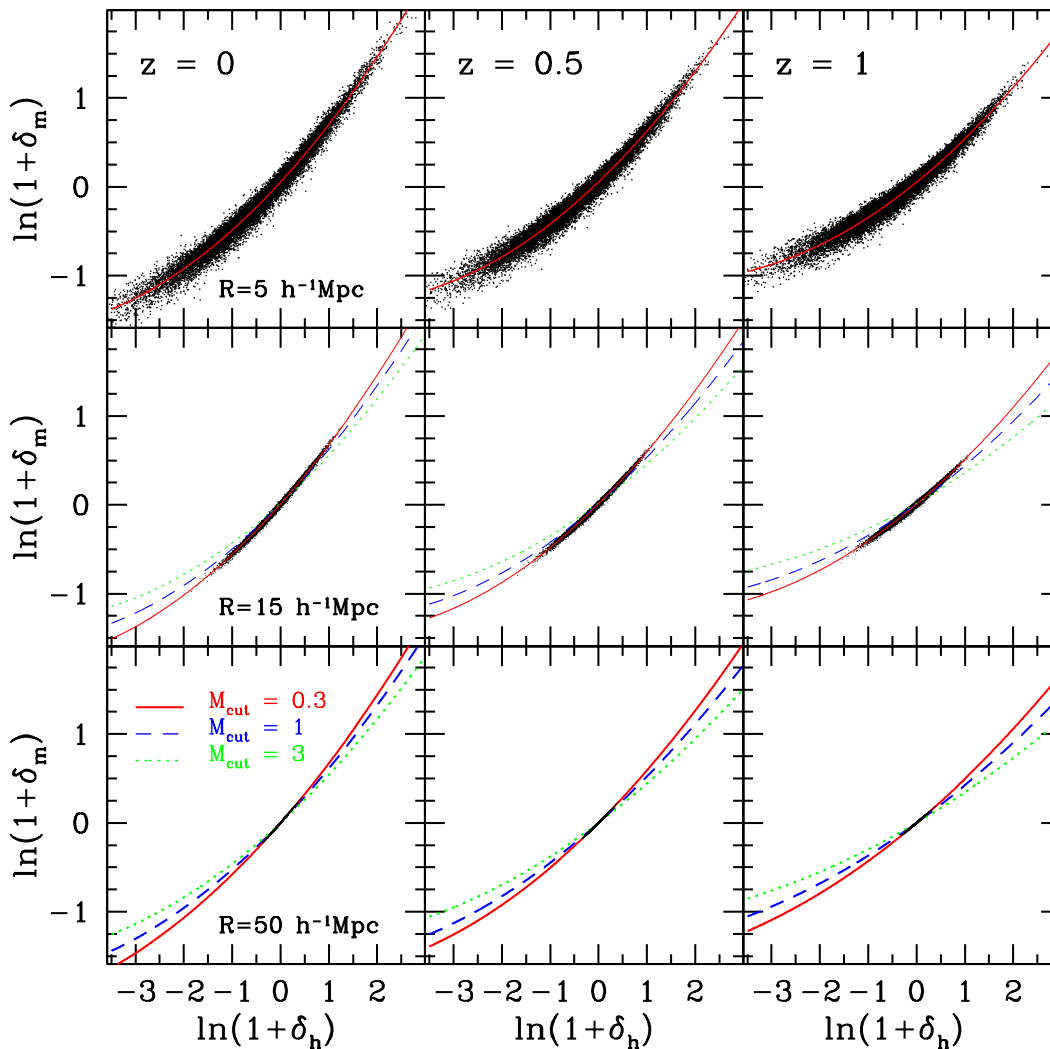


FIG. 2.— The relations between the logarithmic halo mass density and the underlying logarithmic matter density for different mass cuts and smoothing scales at different redshifts. The panels in the first, second and third row are for Gaussian smoothing length of 5, 15 and 50  $h^{-1}\text{Mpc}$ , respectively. Those in the first, second and the third column are the relations at  $z=0, 0.5$  and 1, respectively. Also shown are the relations for the cases of three halo mass cuts of 0.3 (solid line), 1.0 (long-dashed line), and 3.0 (dotted line) in units of  $10^{12}h^{-1}M_{\odot}$  best fit to the data.

We fit the values of  $\beta_i$ 's at  $z = 0$  over the  $R$  ranges from 5 to  $50h^{-1}\text{Mpc}$  and the  $M_{\text{cut}}$  range from  $0.3 \times 10^{12}$  to  $3.0 \times 10^{12}h^{-1}M_{\odot}$  using a routine obtained from <http://www.zunzun.com>. The functional forms of the coefficients we use are

$$\beta_1 = aM_{\text{cut}}^c b^{\frac{1}{R}} + d, \quad (2)$$

$$\beta_2 = \frac{a + bM_{\text{cut}} + cR + dM_{\text{cut}}R}{1 + fM_{\text{cut}} + gR + hM_{\text{cut}}R}, \quad (3)$$

$$\beta_0 = \frac{a + bM_{\text{cut}} + cR + dM_{\text{cut}}R}{1 + f \ln(M_{\text{cut}}) + g \ln(R) + h \ln(M_{\text{cut}}) \ln(R)} + i \quad (4)$$

Table 1 lists the best-fit values of the constants in these functions when the halo mass is in units of  $10^{12}h^{-1}M_{\odot}$ . The parameter values in this table are useful only for the cosmological model we adopted. A simulation using slightly different cosmological parameters would give slightly different  $\beta$ 's. The aim of the current study is to

TABLE 1  
COEFFICIENTS OF THE SECOND-ORDER BIAS MODEL AT REDSHIFT  
 $z = 0$ .

	$a$	$b$	$c$	$d$	$f$	$g$	$h$	$i$
$\beta_1$	-0.297	1.85	1.77	0.87				
$\beta_2$	0.056	7.15E-3	-6.66E-4	-7.32E-5	0.175	-9.39E-3	1.08E-4	
$\beta_0$	1220	11.5	14.5	-0.315	-1310	4490	354	-0.105

show that the mapping from halo mass density to underlying matter density can be well-modeled by a second-order polynomial when logarithmic densities are used.

#### 3.4. Dependence on redshift

We find that the redshift dependence of the  $D_h$ - $D_m$  relation can be accurately modeled through rms value matching of the  $D$  fields across different redshifts. When a second-order  $D_h$ - $D_m$  relation is found at one epoch  $z_1$ , the corresponding equation at a different epoch  $z_2$

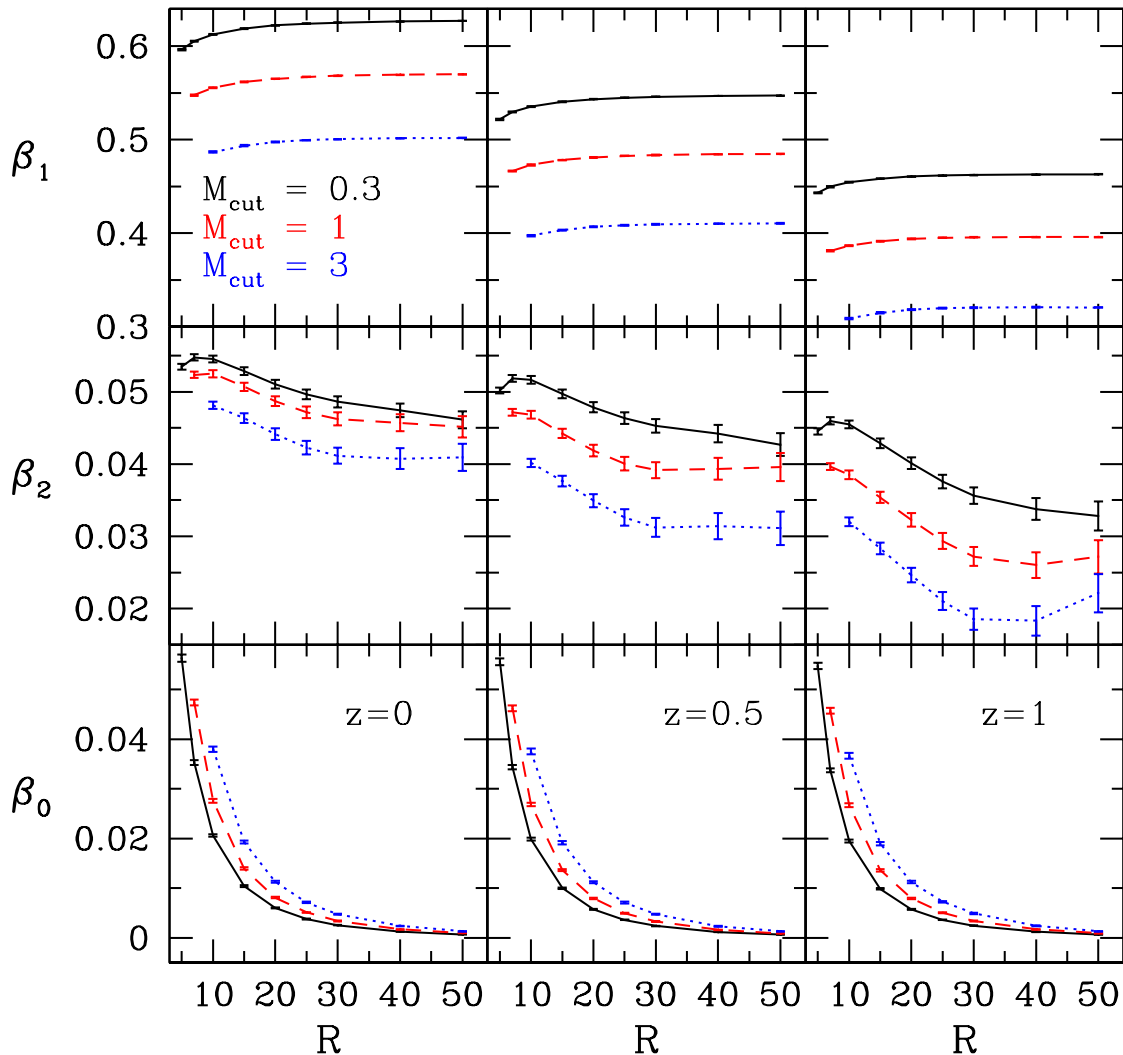


FIG. 3.— The bias factors  $\beta_i$ 's in our second-order halo bias model of the logarithmic density. For each halo masscut of  $0.3 \times 10^{12} h^{-1} M_\odot$  (solid line),  $1 \times 10^{12} h^{-1} M_\odot$  (dashed line) and  $3 \times 10^{12} h^{-1} M_\odot$  (dotted line) the bias factors are given as a function of the Gaussian smoothing radius. The bias factors are inspected at three redshift epochs  $z = 0, 0.5,$  and  $1.0$ .

is accurately given if  $D$ 's are scaled to  $D\sigma_D(z_2)/\sigma_D(z_1)$ . This is demonstrated in Figure 4. It shows the  $D_h$ - $D_m$  relations for  $M_{\text{cut}} = 3 \times 10^{11} h^{-1} M_\odot$  and  $R = 5 h^{-1} \text{Mpc}$  at redshifts  $z = 0$  (dotted line),  $0.5$  (short-dashed line), and  $1.0$  (long-dashed line). The lines for the  $z = 0.5$  and  $1$  cases are drawn by scaling the  $x$  and  $y$ -axes by  $\sigma_D(z)/\sigma_D(0)$ . It can be seen that the lines are very close to one another once the scaling is made. To make Equation (1) applicable at different redshifts we introduce a scaled variable  $\Delta = D\sigma_D(z)/\sigma_D(0)$  and arrive at a modified halo bias model

$$\Delta_m = \beta_0 + \beta_1 \Delta_h + \beta_2 \Delta_h^2, \quad (5)$$

where  $\Delta_m = D_m \sigma_{D_m}(z)/\sigma_{D_m}(0)$  and  $\Delta_h = D_h \sigma_{D_h}(z)/\sigma_{D_h}(0)$ . We emphasize again that the matter density is expanded in terms of the halo mass density in our model.  $\Delta$ 's are equal to  $D$ 's at  $z = 0$ . It is reassuring that the redshift dependence of  $D_h$  versus  $D_m$  relation satisfies this scaling relation down to the smoothing scales as small as  $5 h^{-1} \text{Mpc}$ . This scaling property

of our second-order polynomial bias model also makes the model applicable to cases with a different degree of biasing.

#### 4. STOCHASTICITY

At a particular point in space the halo density is not completely fixed for a given matter density, but can have a range of values as can be seen in Figure 2. This dispersion in the relation is called stochasticity (Seljak et al. 2009). Ue-Li Pen(1998) claimed that on large scales galaxy density variance, galaxy-dark matter density bias, and their cross-correlation coefficient are the only coefficients that are required in determining the dark matter power spectrum, and in mildly nonlinear regime skewness and non-linear bias should come into consideration. Dekel & Lahav(1999) proposed conditional distribution in estimating random fluctuations of galaxy and mass density. They claimed that the scatter in this relation arises from the hidden factors related to shot noise,

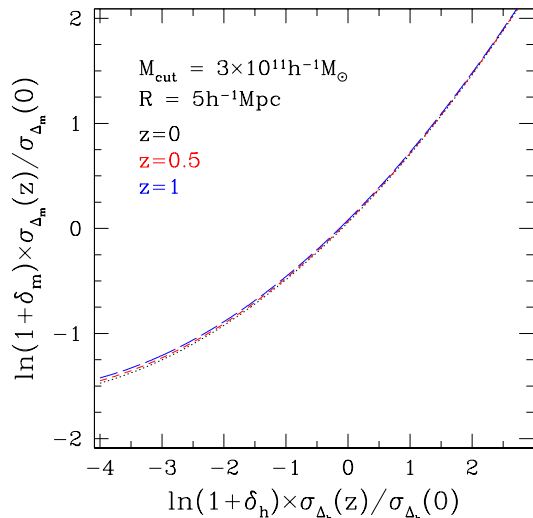


FIG. 4.— The relation between  $D_h = \ln(1 + \delta_h)$  and  $D_m = \ln(1 + \delta_m)$  at redshift  $z = 0$  (dotted line),  $0.5$  (short-dashed) and  $1.0$  (long-dashed). The lines for  $z = 0.5$  and  $1$  are scaled by  $D\sigma(z)/\sigma(0)$ .

galaxy formation etc. Somerville et al. (2001) modeled the non-linear stochastic bias as a combination of mean biasing function and scatter about it. It was claimed that it depends on halo mass, luminosity and scale. They investigated the time dependence of bias in detail, and concluded that the evolution of biasing depends largely on the cosmological model due to the growth rate. Seljak & Warren (2004) estimated the halo bias as approximately constant for halo masses one-tenth below the non-linear mass. They also explored the growth of individual Fourier modes of dark matter density field and found large fluctuations due to non-linearity. Similar large fluctuations were found between modes of halos and dark matter densities, and between modes of halo density fields with different halo mass. In a succeeding study, Bonoli & Pen (2009) tested the validity of basic assumption of halo bias studies that presumes no intrinsic stochasticity between halo and dark matter. From the behavior of stochasticity in the correlation between halos with different mass and between halos and dark matter as a function of mass, they claimed that even on large scales, stochasticity cannot be neglected. Roth & Porciani (2011) tested the third-order standard perturbation theory (SPT) by comparing the dark matter field produced by simulation with the numerically-calculated dark matter field using the SPT from initial conditions, both point-by-point and statistically. They claimed that on large scales above  $8h^{-1}\text{Mpc}$ , they agreed well up to redshift 0. To relate the matter field to halo density fields identified from the simulation, they applied Eulerian bias (ELB) model up to the third order by fitting scatter plots. Using this bias they reconstructed the halo field to show that it cannot reproduce all the detailed properties of halo distribution. On large scales they showed that bias can be approximated as a constant and it agrees with the parameter  $b_1$  from the local bias model, in those regions with  $\delta \ll 1$ . As a consequence they concluded that the SPT is a good method to study the matter field on fairly large smoothing scales, but the ELB model cannot fully reconstruct the halo density field.

Since all the matter in  $\Lambda\text{CDM}$  universes is contained in halos,  $\Delta_h$  is identical to  $\Delta_m$  and the  $\Delta_h$ - $\Delta_m$  relation will be exactly linear when the halo mass cut is zero. Since all the matter in the LCDM universes is contained in halos in the case of a pure N-body simulation, then the stochastic term is thought to be caused by the background uncounted halos with mass below the mass cut. (In practice, the unresolved halos below the mass cut is responsible only for a part of stochasticity since there can be other forms of mass components whose distribution can be governed by various environmental factors.) To reduce the stochasticity Hamaus et al. (2010) suggested a simple halo weighting scheme where the weight to a halo with mass  $M_h$  is not  $M_h$  but  $M_h + M_{\text{cut}}$ . When we implement this weighting scheme into the density calculation, we find the  $\delta_h$ - $\delta_m$  relation slightly changes and its dispersion somewhat decreases. We find the reduction of the scatter is about 10% in the case of  $M_{\text{cut}} = 3 \times 10^{11} M_\odot$  and  $R = 5h^{-1}\text{Mpc}$ . Since the reduction of stochasticity is not significant, we will not adopt this weighting.

We look for a possibility that some local parameters other than the local density have information on the underlying matter density, and a part of the stochasticity in the  $\Delta_h$ - $\Delta_m$  relation is actually not random but can be determined by such environmental parameters. We investigate the dependence of the scatter on a few local and nonlocal physical parameters. They include the gravitational shear tensor  $\partial_i \partial_j \Phi$ , Laplacian of the logarithmic halo density field  $\nabla^2 \Delta$ , and the difference between the densities on two smoothing scales  $\Delta(R_1) - \Delta(R_2)$ . The mass cut is fixed to  $M_{\text{cut}} = 3 \times 10^{11} h^{-1} M_\odot$  in this section.

The halo collapse time and the mass accreted till an epoch can depend on various environmental parameters, and the halos with mass above  $M_{\text{cut}}$  located in the same local density regions can have different physical parameters and the shape of the mass function can depend on environment. For example, the gravitational shear force can influence the halo formation under the same density environment (McDonald & Roy 2009); see also Chan et al. (2012) and Tobias et al. (2012). We calculate the traceless Hessian matrix of the gravitational potential

$$H_{ij} = \frac{\partial^2 \Phi}{\partial x_i \partial x_j} - \frac{1}{3} \delta_{ij} \nabla^2 \Phi \quad (6)$$

from the smooth halo mass density and matter density fields. The traceless Hessian matrix is used to retain only the anisotropic component of the gravitational potential field. Its eigenvalues  $\lambda_i$  are used to define the ellipticity and prolateness parameters

$$e = (\lambda_1 - \lambda_3) / \lambda, \quad (7)$$

$$p = (\lambda_1 - 2\lambda_2 + \lambda_3) / \lambda, \quad (8)$$

where  $\lambda_1 \geq \lambda_2 \geq \lambda_3$  is assumed and the magnitude of the shear tensor  $\lambda = \sqrt{\lambda_1^2 + \lambda_2^2 + \lambda_3^2}$ . The curvature of the gravitational potential field determined the shear tensor, which produces the tidal torque on density fluctuations. The ellipticity and prolateness quantifies the shape of the potential by comparing the size of the curvature in directions of the principal axes, while the shear magnitude gives the size of the curvature itself. The ellipticity and prolateness parameters are divided by the shear magnitude so that only the information on the potential shape can be obtained.



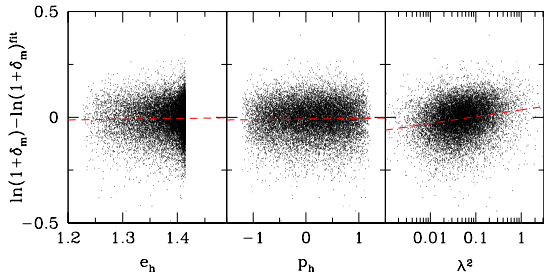


FIG. 5.— The scatter term of  $\ln(1 + \delta_m)$  from the second-order halo bias model as a function of ellipticity, prolateness and shear magnitude calculated from the halo distribution.

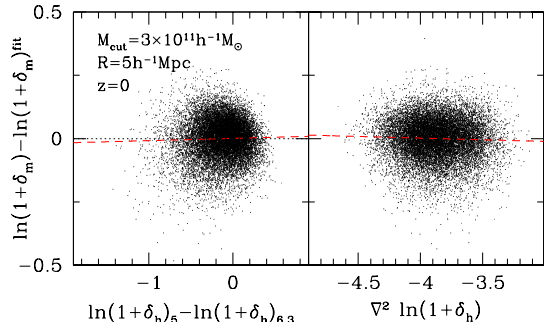


FIG. 6.— The scatter term from the second-order halo bias model versus the difference between  $\Delta_h$  on two smoothing scales (left panel) and the Laplacian of  $\Delta_h$  (right panel).

Figure 5 is the scatter term in  $\ln(1 + \delta_m)$  from the fitting formula shown in Figure 2 (the panel at the upper left corner). It can be seen that the scatter term does not depend on the normalized ellipticity or prolateness parameters, but weakly depends on the shear magnitude. A least-square fit of a line results in

$$\ln(1 + \delta_m) - \ln(1 + \delta_m)_{\text{fit}} = 0.035 + 0.032 \log_{10}(\lambda^2), \quad (9)$$

where the error in the slope is 0.01.

In the left panel of Figure 6 we show the scatter term as a function of the density difference between  $\ln(1 + \delta_h)$  with  $R = 5h^{-1}\text{Mpc}$  and  $6.3h^{-1}\text{Mpc}$ , a measure of non-locality. The smoothing volume in the latter case is twice that of the first case. We do not find a statistically significant dependence of the scatter on the density difference. The right panel shows the scatter term as a function of the Laplacian of the smooth halo mass density. Again there is no significant correlation.

Our results can be compared with the theoretical prediction of McDonald & Roy (2009) who showed that the galaxy density can be Taylor-expanded in terms only of  $\delta_m$ ,  $\delta_m^2$ , and  $\lambda_m^2$  up to the second order. To conclude we find that the scatter term in  $\ln(1 + \delta_m)$  shown in Figure 2 can be partly determined by the magnitude of the gravitational shear tensor, and the halo bias model can be improved to the following formula

$$\Delta_m = \beta_0 + \beta_1 \Delta_h + \beta_2 \Delta_h^2 + d(\lambda), \quad (10)$$

where the extra deterministic term  $d(\lambda)$  is given by Equation (9) for the case of  $M_{\text{cut}} = 3 \times 10^{11} h^{-1} M_{\odot}$  and  $R = 5h^{-1}\text{Mpc}$ . For an observed distribution of dark halos Equation (10) gives the estimate of the underlying matter density field.

## 5. SUMMARY AND DISCUSSION

We present an analytic model for the local bias of dark matter halos simulated in an N-body simulation of the  $\Lambda\text{CDM}$  universe. We found that a second-order polynomial model for the relation between the halo mass distribution and the underlying matter distribution is an excellent fit to N-body simulation data when the logarithmic density is used. The model is second-order not in the matter density, but in the halo mass density. The model remains excellent for all smoothing scales (from  $R = 5h^{-1}\text{Mpc}$  to  $50h^{-1}\text{Mpc}$ ), halo mass cuts (from  $M_{\text{cut}} = 3 \times 10^{11}$  to  $3 \times 10^{12} h^{-1} M_{\odot}$ ), and redshift ranges (from  $z = 0$  to 1.0) considered. The scatter term in the relation between the halo mass density and matter density is found not entirely random. We showed that a fraction of the scatter can be determined by the magnitude of the shear tensor and the scatter can be reduced.

Cen & Ostriker (1993) claimed that the following second-order polynomial relation between matter and galaxies

$$\log\left(\frac{n_g}{\langle n_g \rangle}\right) = A + B \log\left(\frac{\rho_{\text{tot}}}{\langle \rho_{\text{tot}} \rangle}\right) + C [\log\left(\frac{\rho_{\text{tot}}}{\langle \rho_{\text{tot}} \rangle}\right)]^2 \quad (11)$$

was an excellent fit to their simulation results of Cen & Ostriker (1992). Here  $n_g$  is the simulated galaxy number density and  $\rho_{\text{tot}}$  is the total mass density. It should be noted that Equation (11) is completely different from our model even though it also adopted a second-order polynomial of logarithmic density. First, it uses galaxy number density, and it is expected from Figure 1 that the galaxy number density is not related with the total mass density through a simple polynomial. Second, Equation (11) is second-order in log total matter density but our model (Eq. 1) is second-order in the halo mass density and linear in the matter density. We checked Figure 4 of Cen & Ostriker (1992) and found the figure in actual fact supports our model instead of Equation (11).

Manera & Gaztanaga (2011) studied a local bias model of the halo distribution in N-body simulations. However, they also used the halo number density instead of the mass density, and adopted a polynomial model where the halo overdensity is expanded in terms of the matter overdensity up to the second order. The mean separation of the FoF halos they used was  $11h^{-1}\text{Mpc}$  even in the lowest mass halo sample at  $z = 0$ , and their study was reliable only on large smoothing scales of  $R \geq 11h^{-1}\text{Mpc}$  (or cubical cell size  $\geq 28h^{-1}\text{Mpc}$ ). Therefore the data was not quite appropriate for the halo bias study in the non-linear regime. Furthermore, the cubical cell smoothing kernel they used produced a large shot noise in the halo density, which coupled with the true smoothing length dependence of the bias factors.

Recently, Neyrinck et al. (2009, 2011) found that the linear regime in the dark matter power spectrum can be dramatically extended to high  $k$ 's if a logarithmic mapping or a Gaussianization for the density field is made. This is a very useful finding because the size of observational data used for primordial parameter estimation effectively becomes many orders of magnitude larger by simply making such a trivial non-linear transformation. We do not inspect the relation between the matter and halo densities in Fourier space in detail in this paper, but just demonstrate that the linear regime extends to much smaller scales if the logarithmic transformation is made. Neyrinck et al. (2009) showed the same for the

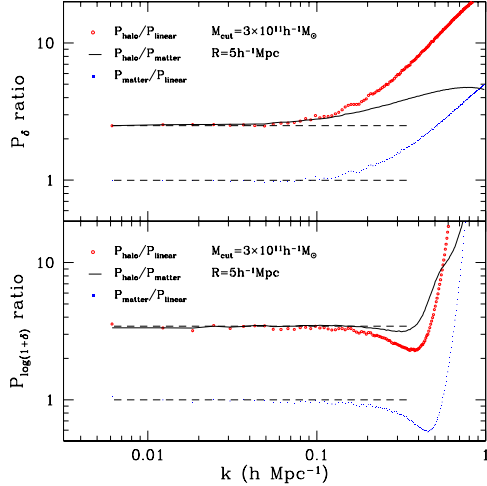


FIG. 7.— The upper panel is the ratio of the power spectrum calculated from the  $\delta$  fields, and the lower panel is the same plot but calculated from the  $\ln(1+\delta)$  field, in Fourier space. Red dots indicate the ratio between the halo power spectrum and matter power spectrum. Blue dots are the ratio between the matter and initial (Gaussian random field) power spectrum to show how the evolved matter field is deviated from the initial power spectrum. The black solid lines are the ratios between the halo and matter power spectra that show the scale-dependent halo biasing in Fourier space. The horizontal lines are constant bias relations.

dark matter field, but we show that the same is true even if the halo mass density field is used.

Each N-body simulation gives the dark matter density down to very small scales, and the log density can be calculated. But in practice, galaxies and dark halos

are much sparser and their spatial distributions should be smoothed to give smooth density fields. To obtain a reliable density estimation we adopt to use a Gaussian smoothing length equal to or greater than the mean halo separation. Figure 7 shows the behavior of the halo bias in terms of the power spectrum of the smoothed halo mass density fields. The black solid line in the upper panel indicates that the halo mass power spectrum ( $P_{\text{halo}} = \langle |\delta_h^2| \rangle$ ) deviates from the linear relation with the dark matter power spectrum  $P_{\text{matter}}$  starting from  $k \approx 0.05 h \text{Mpc}^{-1}$ . However, this scale becomes about  $k \approx 0.2 h \text{Mpc}^{-1}$  as shown in the lower panel when logarithmic values are used. The scale of the nonlinear halo bias is effectively reduced by a factor of about 4. We have calculated this halo bias function using another simulation with the WMAP 5-year cosmological parameters and different random initial conditions, and found this conclusion remains valid. It is expected that the linear-bias regime can be extended to even smaller scales if one can apply a smaller smoothing for a denser sample.

Gaussianization has a similar effect on the density field (Neyrinck et al. 2009, 2011). It should be noted that Gaussianization has long been used for the study of the large-scale topology of galaxy distribution in order to examine the primordial non-Gaussianity (Weinberg et al. 1987; Choi et al. 2010).

This work was supported by a grant from the Kyung Hee University in 2011 (KHU-20100179). We thank Korea Institute for Advanced Study for providing computing resources (KIAS Center for Advanced Computation Linux Cluster System) for this work.

## REFERENCES

- Audit, E., Teyssier, R., & Alimi, J. M. 1998, *A&A*, 333, 779  
 Barnes, J., & Hut, P. 1986, *Nature*, 324, 446  
 Bonoli, S., & Pen, U. L. 2009, *MNRAS*, 396, 1610  
 Cen, R., & Ostriker, J. P. 1992, *ApJ*, 399, L113  
 Cen, R., & Ostriker, J. P. 1993, *ApJ*, 417, 415  
 Chan, K. C., Scoccimarro, R., & Sheth, R. K. arXiv:1201.3614  
 Choi, Y.-Y., Park, C., Kim, J., Gott, J. R., Weinberg, D. H., Vogeley, M. S., & Kim, S. S. 2010, *ApJS*, 190, 181  
 Coles, P., & Jones, B., 1991, *MNRAS*, 248, 1  
 Colombi, S. 1994, *ApJ*, 435, 301  
 Davis, M., Efstathiou, G., Frenk, C. S., & White, S. D. M. 1985, *ApJ*, 292, 371  
 Davis, M. & Peebles, P. J. E., 1983, *ApJ*, 267, 465  
 Dekel, A. & Lahav, O. 1999, *ApJ*, 520, 24  
 Dubinski, J., Humble, R., Pen, U. L., Laken, C., & Martin, P. 2003, astro-ph/0305109v1  
 Dubinski, J., Kim, J., Park, C., & Humble, R. 2004, *New Astronomy*, 9, 111  
 Eisenstein, D. J. & Hu, W. 1998, *ApJ*, 496, 605  
 Fry, J. N., & Gaztanaga, E. 1993, *ApJ*, 413, 447  
 Gott, J. R., Choi, Y.-Y., Park, C., & Kim, J. 2009, *ApJ*, 695, L45  
 Gramann, M., Cen, R., & Gott, J. R. 1994, *ApJ*, 425, 382  
 Guo, H. & Jing, Y. P. 2009, *APJ*, 702, 425  
 Hamaus, N., Seljak, U., Desjacques, V., Smith, R. E., & Baldauf, T. 2010, *Phys. Rev. D*, 82, 3515  
 Hwang, H. S., & Park, C. 2009, *ApJ*, 700, 791  
 Kayo, I., Taruya, A., & Suto, Y. 2001, *ApJ*, 561, 22  
 Kim, J. & Park, C. 2006, *ApJ* 639, 600  
 Kim, J., Park, C., & Choi, Y.-Y. 2008, *ApJ*, 683, 123  
 Manera, M., & Gaztanaga, E. 2011, *MNRAS*, 415, 393  
 Marinoni, C., Hudson, M. J., & Giuricin, G. 2002, *ApJ*, 569, 91  
 McDonald, P., & Roy, A. 2009, *JCAP*, 8, 20  
 Neyrinck, M. C., Szapudi, I., & Szalay, A. S. 2011, *ApJ*, 731, 116  
 Neyrinck, M. C., Szapudi, I., & Szalay, A. S. 2009, *ApJ*, 698, L90  
 Park, C. 1990, *MNRAS*, 242, 59  
 Park, C., Vogeley, M. S., Geller, M. J., & Huchra, J. P. 1994, *ApJ*, 431, 569  
 Park, C. 1997, *JKAS*, 30, 191  
 Park, C., Choi, Y.-Y., Vogeley, M. S., Gott, J. R., Kim, J., Hikage, C., Matsubara, T., Park, M.-G., Suto, Y., & Weinberg, D. H. 2005, *ApJ*, 633, 11  
 Park, C., Gott, J. R., & Choi, Y.-Y. 2008, *ApJ*, 674, 784  
 Park, C. & Choi, Y.-Y. 2009, *ApJ*, 691, 1828  
 Park, C. & Hwang, H. S. 2009, *ApJ*, 699, 1595  
 Park, H., Kim, J., & Park, C. 2010, *ApJ*, 714, 207  
 Pen, U. L. 1998, *ApJ*, 504, 601  
 Pollack, J. E., Smith, R. E. & Porciani, C. 2012, *MNRAS*, 000, 000  
 Roth, N. & Porciani, C. 2011, *MNRAS*, 415, 829  
 Seljak, U., Hamaus, N., & Desjacques, V. 2009, *Phys. Rev. Letters*, 103, 091303  
 Seljak, U. & Warren, M. S. 2004, *MNRAS*, 355, 129  
 Shankar, F., Lapi, A., Salucci, P., Zotti, G. D., & Danese, L. 2006, *ApJ*, 643, 14  
 Smith, R. E., Scoccimarro, R., & Sheth, R. K. 2007, astro-ph/0609547v3  
 Somerville, R. S., Lemson, G., Sigard, Y., Dekel, A., Kauffmann, G., & White, S. D. M. 2001, *MNRAS*, 320, 289  
 Spergel, D. N., et al. 2007, *ApJS*, 170, 377  
 Tegmark, M., et al. 2006, *Phys. Rev. D*, 74, 123507  
 Tobias, B., Uros, S., Desjacques, V., & McDonald, P. 2012, arXiv:1201.4827  
 Vale, A., & Ostriker, J. P. 2004, *MNRAS*, 353, 189  
 Vale, A., & Ostriker, J. P. 2006, *MNRAS*, 371, 1173  
 Weinberg, D. H., Gott, J. R., & Melott, A. L. 1987, *ApJ*, 321, 2  
 White, S. D. M. & Rees, M. 1978, *MNRAS*, 183, 341